

## Chapter 8

# Deterministic Compartmental Models

*This is Polyfemos the copper Cyclops whose body is full of water and someone has given him one eye, one mouth and one hand to each of which a tube is attached. Water appears to drip from his body and to gush from his mouth, all the tubes have regular flow. When the tube connected to his hand is opened his body will empty within 3 days, while the one from his eye will empty in one day and the one from his mouth in 2/5 of a day. Who can tell me how much time is needed to empty him when all three are opened together?*

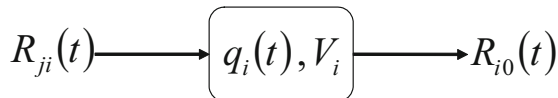
Metrodorus (331-278 BC)

Compartmental modeling is a broad modeling strategy that has been used in many different fields, though under varying denominations. Virtually all current applications and theoretical research in compartmental analysis are based on deterministic theory. In this chapter deterministic compartmental models will be presented. The concept of compartmental analysis assumes that a process may be divided though it were occurring in homogeneous components, or “compartments.” Various characteristics of the process are determined by observing the movement of material. A compartmental system is a system that is made up of a finite number of compartments, each of which is homogeneous and well mixed, and the compartments interact by exchanging material. Compartmental systems have been found useful for the analysis of experiments in many branches of biology.

We assume that compartment  $i$  is occupied at time 0 by  $q_{i0}$  amount of material and we denote by  $q_i(t)$  the amount in the compartment  $i$  at time  $t$ . We also assume that no material enters the compartments from the outside of the compartmental system and we denote by  $R_{i0}(t)$  the rate of elimination from compartment  $i$  to the exterior of the system. Let also  $R_{ji}(t)$  be the transfer rate of material from the  $j$ -th to  $i$ -th compartment. Because the material is distributed in each compartment at uniform concentration, we may assume that each compartment occupies a constant volume of distribution  $V_i$ . The box in Figure 8.1 represents the  $i$ -th compartment of a system of  $m$  compartments.

Mathematics is now called upon to describe the compartmental configurations and then to simulate their dynamic behavior. To build up mathematical equations

**Fig. 8.1** The rates of transfer for the  $i$ -th compartment



expressing compartmental systems, one has to express the mass balance equations for each compartment  $i$ :

$$\dot{q}_i(t) = -R_{i0}(t) + \sum_{\substack{j=1 \\ j \neq i}}^m R_{ji}(t), \quad (8.1)$$

with initial condition  $q_i(0) = q_{i0}$ . Thus, we obtain  $m$  differential equations, one for each compartment  $i$ .

## 8.1 Linear Compartmental Models

Now, some fundamental hypotheses, commonly called laws, were employed to expand the transfer rates appearing in (8.1). Fick's law is largely used in current modeling (cf. Section 2.3 and equation 2.14). It assumes that the transfer rate of material by diffusion between regions  $l$  (left) and  $r$  (right) with concentrations  $c_l$  and  $c_r$ , respectively, is

$$R_{lr}(t) = -CL_{lr}(c_r - c_l). \quad (8.2)$$

This law may be applied to the transfer rates  $R_{ji}(t)$  of the previous equation for all pairs  $j$  and  $i$  of compartments corresponding to  $l$  and  $r$  and for the elimination rate  $R_{i0}(t)$ , where the concentration is assumed nearly zero in the region outside the compartmental system. One has for the compartment  $i$ ,

$$\dot{q}_i(t) = -CL_{i0}c_i(t) + \sum_{\substack{j=1 \\ j \neq i}}^m CL_{ji}[c_j(t) - c_i(t)],$$

where  $CL_{i0}$  is the *total clearance* from compartment  $i$  and  $CL_{ji}$  is the *intercompartmental clearance* between  $i$  and  $j$ . We recall that the clearance has a bidirectional property ( $CL_{ji} = CL_{ij}$ ) and the subscript  $ij$  denotes simply the pair of compartments referenced. The initial condition associated with the previous differential equation is denoted by  $q_i(0) = q_{i0}$ . Using the volumes of distribution  $V_i$  and the well-known relationship  $q_i(t) = V_i c_i(t)$ , we substitute the concentrations with the corresponding amounts of material:

$$\dot{q}_i(t) = -k_{i0}q_i(t) + \sum_{\substack{j=1 \\ j \neq i}}^m k_{ji}q_j(t) - \sum_{\substack{j=1 \\ j \neq i}}^m k_{ij}q_i(t).$$

The constants  $k$  are called the *fractional flow rates*. They have the dimension of  $\text{time}^{-1}$  and they are defined as follows:

$$\frac{CL_{i0}}{V_i} \triangleq k_{i0}, \quad \frac{CL_{ij}}{V_i} \triangleq k_{ij}, \quad \frac{CL_{ij}}{V_j} \triangleq k_{ji}. \quad (8.3)$$

In contrast to the clearance, the fractional flow rates indicate the flow direction, i.e.,  $k_{ji} \neq k_{ij}$ , the first subscript denoting the start compartment, and the second one, the ending compartment. The fractional flow rates and the volumes of distribution are usually called *microconstants*.

When the volume of the compartment being cleared is constant, the assumption that the fractional flow rate is constant is equivalent to assuming that the clearance is constant. But in the general case, in which the volume of distribution cannot be assumed constant, the use of fractional flow rates  $k$  is unsuitable, because the magnitude of  $k$  depends as much upon the volume of the compartment as it does upon the effectiveness of the removal process. In contrast, the clearance depends only upon the overall effectiveness of removal, and can be used to characterize any removal process whether it be constant or changing, capacity-limited or supply-limited [339].

Through the following procedure the equations for a deterministic model can be obtained:

1. Represent the underlying mechanistic model with the desired physiological structure through a set of phenomenological compartments with their interconnections.
2. For each compartment in the configuration, apply the mass balance law to obtain the differential equation expressing the variation of amount per unit of time. In these expressions, constant or variable fractional flow rates  $k$  can be used.
3. Solve the system of differential equations obtained for all the compartments by using classical techniques or numerical integration (e.g., Runge–Kutta) [340].

Therefore, Fick's law, when applied to all elements of the compartmental structure, leads to a system of linear differential equations. There are as many equations as compartments in the configuration. If we set

$$k_{ii} = k_{i0} + \sum_{\substack{j=1 \\ j \neq i}}^m k_{ij},$$

the equation for the  $i$ -th compartment is

$$\dot{q}_i(t) = -k_{ii}q_i(t) + \sum_{\substack{j=1 \\ j \neq i}}^m k_{ji}q_j(t), \quad (8.4)$$

associated with initial conditions  $q_{i0}$ . In the previous equation, the  $q_i(t)$  and  $q_{i0}$  amounts of material can be compiled in vector forms as  $\underline{q}(t)$  and  $\underline{q}_0$ , respectively. In the same way, the fractional flow rates  $k_{ij}$  may be considered as the  $(i,j)$ -th elements of the  $m \times m$  fractional flow rates matrix  $\mathbf{K}$ . Thus, the set of linear differential equations can be expressed as

$$\dot{\underline{q}}^T(t) = \underline{q}^T(t) \mathbf{K},$$

and having the following solution:

$$\underline{q}^T(t) = \underline{q}_0^T \exp(\mathbf{K}t), \quad (8.5)$$

where the initial conditions are *postmultiplied* by  $\exp(\mathbf{K}t)$ , which is defined by

$$\exp(\mathbf{K}t) \triangleq \mathbf{I} + \sum_{i=1}^{\infty} \frac{\mathbf{K}^i t^i}{i!}.$$

In most pharmacokinetic applications, one can assume that the system is open and at least weakly connected. This is the case of mammillary compartmental models, where the compartment no.1 is referred to as the *central compartment* and the other compartments are referred to as the *distribution compartments*, characterized by  $k_{i0} = 0$  and  $k_{ij} = 0$  for  $i, j = 2 : m$ . For open mammillary compartmental configurations, the eigenvalues of  $\mathbf{K}$  are distinct, real, and negative, implying that

$$q_i(t) = \sum_{j=1}^m B_{ij} \exp(-b_j t),$$

the so-called formula of *sum of exponentials*, which is common in pharmacokinetics. The  $B_{ij}$  and positive  $b_j$  are often called *macroconstants*, and they are functions of the microconstants. The equations relating these formulations are given explicitly for the common two- and three-compartment models in many texts [332, 341]. It should be noted, however, that the addition of a few more compartments usually complicates the analysis considerably.

## 8.2 Routes of Administration

In practice, it is unlikely to have compartmental models with initial conditions unless there are residual concentrations obtained from previous administrations. Drugs are administered either by extravascular, or intravascular in single or repeated experiments. Extravascular routes are oral, or intramuscular routes, and intravascular are the constant rate short- and long-duration infusions.

- For the extravascular route, the rate of administration is

$$u_{ev}(t) = q_0 k_a \exp(-k_a t),$$

where  $q_0$  is the amount of material initially given to the extravascular site of administration and  $k_a$  is the fractional flow rate for the passage of material from the site of administration toward the recipient compartment;  $k_a$  is the absorption rate constant.

- For the intravascular route with constant rate, we have

$$u_{iv}(t) = \frac{q_0}{T_E - T_S} [H(t - T_S) - H(t - T_E)],$$

where  $q_0$  is the amount of material given at a constant rate in the venous compartment between the starting time  $T_S$  and the ending time  $T_E$ . Here,  $H(t)$  is the step Heaviside function.

Extravascular and intravascular routes can be conceived as concomitant or repeated, e.g., delayed oral intake with respect to an intramuscular administration, or piecewise constant rate infusions, etc. Applying the superposition principle, the contribution of all administration routes in the same recipient compartment is given by the following input function:

$$u(t) = \sum_{i=1}^{m_{ev}} q_{0i} k_{ai} \exp[-k_{ai}(t - T_i)] + \sum_{i=1}^{m_{iv}} \frac{q_{0i}}{T_{Ei} - T_{Si}} [H(t - T_{Si}) - H(t - T_{Ei})],$$

where the  $m_{ev}$  and  $m_{iv}$  administrations preceding the time  $t$  are associated with the  $q_{0i}$  amounts of material.  $T_i$  is the time of the  $i$ -th extravascular administration, and  $T_{Si}$  and  $T_{Ei}$  are the starting and ending times in the  $i$ -th intravascular administration. The contribution of the input function  $u(t)$  in the mass balance differential equation for the recipient compartment is represented by an additive term in the right-hand side of (8.1).

### 8.3 Time–Concentration Profiles

In (8.4), by dividing the amounts  $q_i(t)$  by non-time-dependent volumes of distribution  $V_i$ , one obtains the differential equations for the concentrations  $c_i(t)$ :

$$\dot{c}_i(t) = -k_{ii}c_i(t) + \sum_{\substack{j=1 \\ j \neq i}}^m \frac{V_j}{V_i} k_{ji}c_j(t). \quad (8.6)$$

Additional assumptions further reduce the complexity of these equations. One such assumption is the incompressibility of the volumes of distribution or, as usually known, the *flow conservation*. This assumption applied to compartment  $j$  leads to

$$\sum_{\substack{i=1 \\ i \neq j}}^m V_i k_{ij} = V_j \sum_{\substack{i=1 \\ i \neq j}}^m k_{ji}.$$

In the special case of a mammillary compartmental configuration, the above relation allows one to express the volume of distribution in peripheral compartments as functions of the fractional flow rates and the volume of distribution of the central compartment  $V_j = [k_{1j}/k_{j1}] V_1$  for  $j = 2 : m$ . Substituting this relationship in (8.6), we obtain

$$\dot{c}_i(t) = -k_{ii}c_i(t) + \sum_{\substack{j=1 \\ j \neq i}}^m k_{ij}c_j(t).$$

This set of linear differential equations can be expressed as  $\dot{\underline{c}}(t) = \mathbf{K}\underline{c}(t)$ , and it has the following solution:

$$\underline{c}(t) = \exp(\mathbf{K}t)\underline{c}_0,$$

where the initial conditions are *premultiplied* by  $\exp(\mathbf{K}t)$  (instead of the *postmultiplication* in the case of amounts; cf. equation 8.5).

These equations are widely used to simulate simple or complex compartmental systems and currently to identify pharmacokinetic systems from observed time–concentration data. However, it is not always possible to write the equations in terms of concentrations that represent true physical blood or plasma levels. In practice, it may occur that some, say two, compartments exchange so rapidly on the time scale of an experiment that they are not distinguishable but merge kinetically into one compartment. If the two compartments represent material that exists at different concentrations in two different spaces, or two forms of a compound in one space, the calculated concentration may not correspond to any actual measurable concentration and thus may be misleading. For this reason the development of differential equations in terms of compartment amounts  $q_i(t)$  is more general. If these equations are available, it is not difficult to convert to concentrations  $c_i(t)$  by assuming that  $V_i$  is a proportionality constant, called the *apparent volume of distribution*, and to solve the equations as long as the volumes are constant in time [342]. If the volumes are changing the problem becomes more difficult.

## 8.4 Random Fractional Flow Rates

The deterministic model with random fractional flow rates may be conceived on the basis of a deterministic transfer mechanism. In this formulation, a given replicate of the experiment is based on a particular realization of the random fractional flow

rates and/or initial amounts  $\Theta$ . Once the realization is determined, the behavior of the system is deterministic. In principle, to obtain from the assumed distribution of  $\Theta$  the distribution of  $q_i(t)$ ,  $i = 1 : m$ , the common approach is to use the classical procedures for transformation of variables. When the model is expressed by a system of differential equations, the solution can be obtained through the theory of random differential equations [343–345]. However, in practice, one can find the moments directly using conditional expectations (cf. Appendix D):

$$E[q_i(t)] = E_{\Theta}[q_i(t | \Theta)],$$

$$\text{Var}[q_i(t)] = \text{Var}_{\Theta}[q_i(t | \Theta)].$$

Besides the deterministic context, the predicted amount of material is subjected now to a variability expressed by the second equation. This expresses the random character of the fractional flow rate, and it is known as *process uncertainty*. Extensive discussion of these aspects will be given in Chapter 11.

#### Example 4. One-Compartment Model

As an illustration of the procedure, consider the one-compartment model  $q(t) = q_0 \exp(-kt)$ . Assuming that  $k$  has a gamma distribution  $k \sim \text{Gam}(\lambda, \mu)$ , one has the solutions

$$E[q(t)] = q_0 E[\exp(-kt)] = q_0 (1 + t/\lambda)^{-\mu},$$

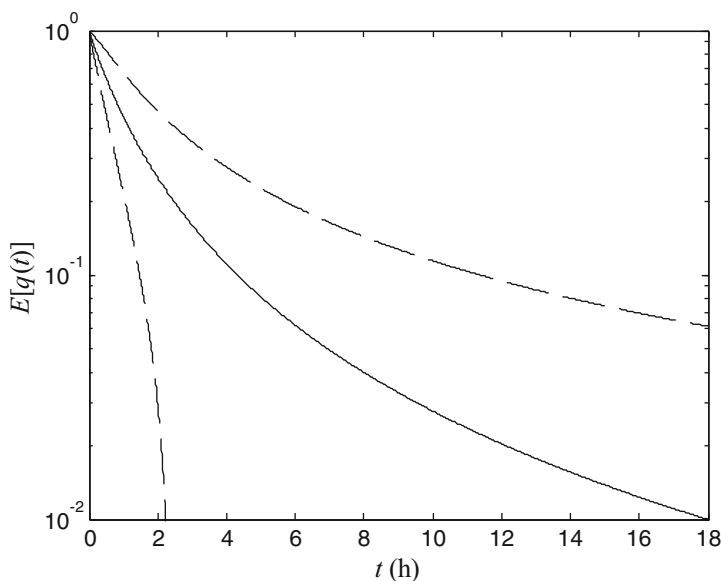
$$\text{Var}[q(t)] = q_0^2 \text{Var}[\exp(-kt)] = q_0^2 \left[ (1 + 2t/\lambda)^{-\mu} - (1 + t/\lambda)^{-2\mu} \right].$$

Figure 8.2 shows  $E[q(t)]$  and  $E[q(t)] \pm \sqrt{\text{Var}[q(t)]}$  with  $q_0 = 1$  and  $k \sim \text{Gam}(2, 2)$ . It is noteworthy that confidence intervals are present due to the variability of the fractional flow elimination rate  $k$ . This variability is inherent to the process and completely different from that introduced by the measurement devices. ■

## 8.5 Nonlinear Compartmental Models

Many systems of interest are actually nonlinear:

- A first formulation considers the transfer rates of material from compartment  $i$  to  $j$  as functions of the amounts in all compartments  $\underline{q}(t)$  and of time  $t$ , i.e.,  $R_{ij}[\underline{q}(t), t]$ . In this case,  $R_{ij}(t)$  in (8.1) should be substituted with  $R_{ij}[\underline{q}(t), t]$ . If we expand the  $R_{ij}[\underline{q}(t), t]$  in a Taylor series of  $\underline{q}(t)$  and retain only the linear terms, the nonlinear transfer rates take the form  $k_{ij}(t) q_i(t)$  and one obtains a linear time-varying compartmental model.



**Fig. 8.2** One-compartment model with gamma-distributed elimination flow rate  $k \sim \text{Gam}(2, 2)$ . The *solid line* represents the expected profile  $E[q(t)]$ , and *dashed lines*, the confidence intervals  $E[q(t)] \pm \sqrt{\text{Var}[q(t)]}$

- A second formulation considers the fractional flow rate of material as a function of  $\underline{q}(t)$  and  $t$ , i.e.,  $k_{ij}[\underline{q}(t), t]$ . In this case,  $k_{ij}$  in (8.4) should be substituted with  $k_{ij}[\underline{q}(t), t]$ .

Therefore, the transfer rates and the fractional flow rates are functions of the vector  $\underline{q}(t)$  and  $t$ . The dependence on  $t$  may be considered as the exogenous environmental influence of some fluctuating processes. If no environmental dependence exists, it is more likely that the transfer rates and the fractional flow rates depend only on  $\underline{q}(t)$ . Nevertheless, since  $\underline{q}(t)$  is a function of time, the observed data in the inverse problem can reveal only a time dependency of the transfer rate, i.e.,  $R_{ij}(t)$ , or of the fractional flow rate, i.e.,  $k_{ij}(t)$ . Hence, the dependency of  $R_{ij}(t)$  and  $k_{ij}(t)$  on  $\underline{q}(t)$  is obscured, and a second-level modeling problem now arises, i.e., how to regress the observed dependency on the  $\underline{q}(t)$  and  $t$  separately. This problem is mentioned in Section 7.7.

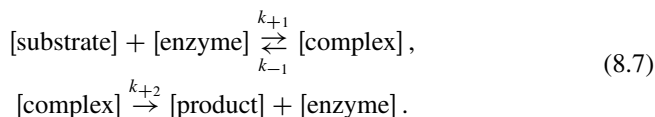
Until now, the compartmental model was considered as consisting of compartments associated with several anatomical locations in the living system. The general definition of the compartment allows us to associate in the same location a different chemical form of the original molecule administered into the process. In other words, the compartmental analysis can include not only diffusion phenomena but also chemical reaction kinetics.

One source of nonlinear compartmental models is processes of enzyme-catalyzed reactions that occur in living cells. In such reactions, the reactant combines with

an enzyme to form an enzyme–substrate complex, which can then break down to release the product of the reaction and free enzyme or can release the substrate unchanged as well as free enzyme. Traditional compartmental analysis cannot be applied to model enzymatic reactions, but the law of mass balance allows us to obtain a set of differential equations describing mechanisms implied in such reactions. An important feature of such reactions is that the enzyme is sometimes present in extremely small amounts, the concentration of enzyme being orders of magnitude less than that of substrate.

### 8.5.1 The Enzymatic Reaction

The mathematical basis for enzymatic reactions stems from work done by Michaelis and Menten in 1913 [346]. They proposed a situation in which a substrate reacts with an enzyme to form a complex, one molecule of the enzyme combining with one molecule of the substrate to form one molecule of complex. The complex can dissociate into one molecule of each of the enzyme and substrate, or it can produce a product and a recycled enzyme. Schematically, this can be represented by



In this formulation  $k_{+1}$  is the rate parameter for the forward enzyme–substrate reaction,  $k_{-1}$  is the rate parameter for the backward reaction, and  $k_{+2}$  is the rate parameter for the creation of the product.

Let  $s(t)$ ,  $e(t)$ ,  $c(t)$ , and  $w(t)$  be the amounts of the four species in the reaction (8.7), and  $s_0$  and  $e_0$  the initial amounts for substrate and enzyme, respectively. The differential equations describing the enzymatic reaction,

$$\begin{aligned} \dot{s}(t) &= -k_{+1}s(t)[e_0 - c(t)] + k_{-1}c(t), & s(0) &= s_0, \\ \dot{c}(t) &= k_{+1}s(t)[e_0 - c(t)] - (k_{-1} + k_{+2})c(t), & c(0) &= 0, \\ \dot{w}(t) &= k_{+2}c(t), & w(0) &= 0, \end{aligned} \quad (8.8)$$

are obtained by applying the law of mass balance for the rates of formation and/or decay, and the conservation law for the enzyme,  $e_0 = e(t) + c(t)$ .

Relying on a suggestion by Segel [347], we make the variables of the above equations dimensionless

$$\begin{aligned} x(\tau) &= \frac{s(t)}{s_0}, & y(\tau) &= \frac{c(t)}{e_0}, & z(\tau) &= \frac{w(t)}{s_0}, \\ \lambda &= \frac{k_{+2}}{k_{+1}s_0}, & \kappa &= \frac{k_{-1} + k_{+2}}{k_{+1}s_0}, & \varepsilon &= \frac{s_0}{e_0}, \end{aligned}$$

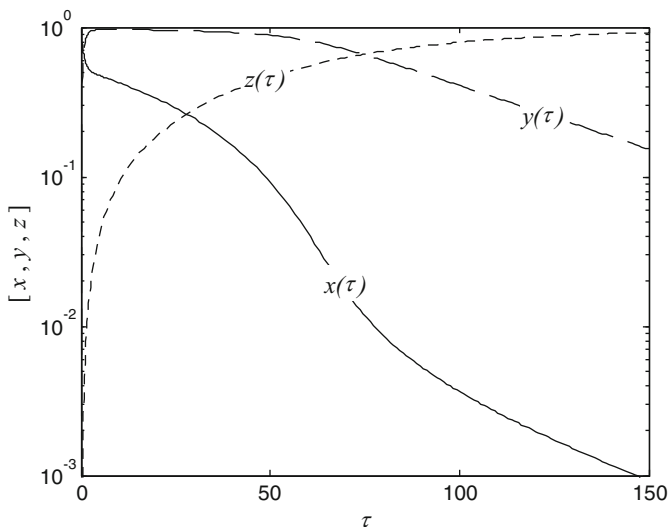


**Fig. 8.3** Profiles of dimensionless reactant amounts, substrate  $x(\tau)$ , complex  $y(\tau)$ , and product  $z(\tau)$

with  $\tau = k_{+1}e_0t$  and  $\kappa \geq \lambda$ . The set of differential equations becomes

$$\begin{aligned} \dot{x}(\tau) &= -x(\tau)[1 - y(\tau)] + (\kappa - \lambda)y(\tau), & x(0) &= 1, \\ \dot{y}(\tau) &= \varepsilon \{x(\tau)[1 - y(\tau)] - \kappa y(\tau)\}, & y(0) &= 0, \\ \dot{z}(\tau) &= \lambda y(\tau), & z(0) &= 0. \end{aligned}$$

This system cannot be solved exactly, but numerical methods easily generate good solutions. The time courses for all reactant species of reaction (8.7) generated from the previous equations with  $(\kappa, \lambda) = (0.015, 0.010)$  and  $\varepsilon = 2$  are shown in the semilogarithmic plot of Figure 8.3. We note that:

- The substrate  $x(\tau)$  drops from its initial condition value, equal to 1, at a rapid rate, but quickly decelerates. Progressively, and for  $\tau > 50$ , the substrate decreases rapidly in a first phase and then slowly, in a second phase. This irregular profile of substrate in the semilogarithmic plot is reflected as a *concavity* or *nonlinearity*, as it is usually called.
- The intermediate compound complex  $y(\tau)$  reaches a maximum (called *quasi-steady state* in biology) that persists only for a time period and then decreases; this time period corresponds to the period of nonlinearity for the substrate time course. In fact, saturation of the complex form is responsible for the nonlinearity in the substrate time course. During this period, there is no free enzyme to catalyze the substrate conversion toward the product.
- The product  $z(\tau)$  reaches the maximum plateau level asymptotically. In contrast to the substrate profile, the nonlinear behavior along the saturation of the complex is not easily defined on the product profile.

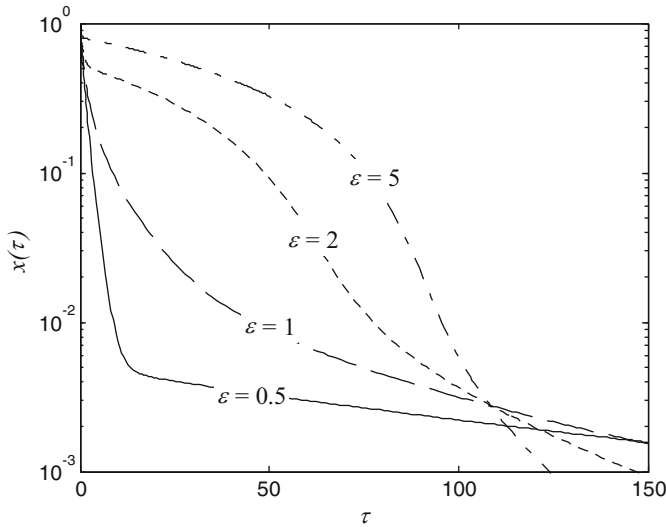


**Fig. 8.4** Influence of  $\varepsilon$  on the substrate  $x(\tau)$  profiles with fixed  $(\kappa, \lambda) = (0.015, 0.010)$  and  $\varepsilon = (0.5, 1, 2, 5)$

Figure 8.4 shows the influence of  $\varepsilon$  on the  $x(\tau)$  shape. For fixed  $(\kappa, \lambda)$ , we simulated the time courses for  $\varepsilon = 0.5, 1, 2, 5$ . It is noted that the shape of the substrate profiles varies remarkably with the values of  $\varepsilon$ ; thus profiles of biphasic, power-law, and nonlinear type are observed. So, the sensitivity of the kinetic profile regarding the available substrate and enzyme amounts is studied by using several  $\varepsilon$  values: for low substrate or high enzyme amounts the process behaves according to two decaying convex phases, in the reverse situation the kinetic profile is concave, revealing nonlinear behavior.

Other processes that lead to nonlinear compartmental models are processes dealing with transport of materials across cell membranes that represent the transfers between compartments. The amounts of various metabolites in the extracellular and intracellular spaces separated by membranes may be sufficiently distinct kinetically to act like compartments. It should be mentioned here that Michaelis–Menten kinetics also apply to the transfer of many solutes across cell membranes. This transfer is called *facilitated diffusion* or in some cases *active transport* (cf. Chapter 2). In facilitated diffusion, the substrate combines with a membrane component called a carrier to form a carrier–substrate complex. The carrier–substrate complex undergoes a change in conformation that allows dissociation and release of the unchanged substrate on the opposite side of the membrane. In active transport processes not only is there a carrier to facilitate membrane crossing, the carrier mechanism is somehow coupled to energy dissipation so as to move the transported material up its concentration gradient.

## 8.6 Complex Deterministic Models

The branching pattern of the vascular system and the blood flow through it has continued to be of interest to anatomists, physiologists, and theoreticians [4, 348, 349]. The studies focusing on the geometric properties such as lengths, diameters, generations, orders of branches in the pulmonary, venular, and arterial tree of mammals have uncovered the principles on which these properties are based. Vascular trees seem to display roughly the same dichotomous branching pattern at different levels of scale, a property found in fractal structures [350–352]. The hydrodynamics of blood flow in individual parts of the dichotomous branching network have been the subject of various studies. Recently, West et al. [353], relying on an elegant combination of the dynamics of energy transport and the mathematics of fractal geometry, developed a hydrodynamic model that describes how essential materials are transported through space-filling fractal networks of branching tubes.

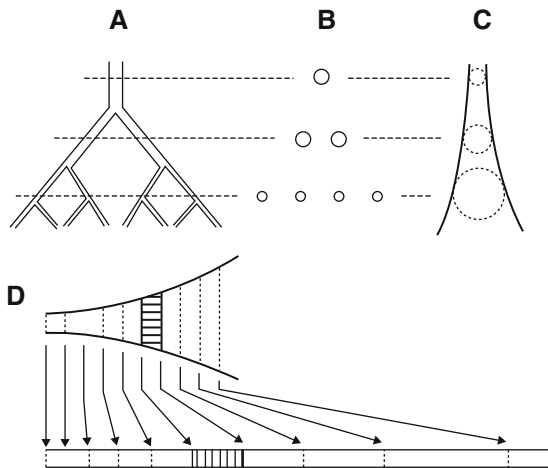
Although these advances provide an analysis of the scaling relations for mammalian circulatory systems, models describing the transport of materials along the entire fractal network of the mammalian species are also needed. Pharmacokinetics and toxicokinetics, the fields in which this kind of modeling is of the greatest importance, are dominated by the concept of homogeneous compartments [354]. Physiologically based pharmacokinetic models have also been developed that define the disposition patterns in terms of physiological principles [282, 354, 355]. The development of models that study the heterogeneity of the flow and the materials distribution inside vascular networks and individual organs has also been fruitful in the past years [294, 356–358]. Herein, we present a simple model for the heterogeneous transport of materials in the circulatory system of mammals, based on a single-tube convection–dispersion system that is equivalent to the fractal network of the branching tubes.

### 8.6.1 Geometric Considerations

We consider a fractal arterial tree that consists of several branching levels where each level consists of parallel vessels, Figure 8.5A. Each vessel is connected to  $m$  vessels of the consequent branching level [353]. We make the assumption that the vessel radii and lengths at each level  $k$  follow a distribution around the mean values  $\rho_k$  and  $\mu_k$ , respectively. The variance of the vessel radii and lengths at each level produces heterogeneity in the velocities.

The total flow across a section of the entire tree is constant (conservation of mass). This allows us to replace the tree with a single one-dimensional tube. Since the tree is not area-preserving and the area of the cross section of the tube is equal to the total area of the cross sections of each level of the tree, the total cross-sectional area of subsequent levels increases, i.e., the tube is not cylindrical (Figure 8.5A–C).

**Fig. 8.5** (A) Schematic representation of the dichotomous branching network. (B) Cross sections at each level. (C) Single tube with continuously increasing radius. (D) Volume-preserving transformation of the varying radius tube to a fixed radius tube. Reprinted from [359] with permission from Springer



Based on the scaling properties of the fractal tree, the noncylindrical tube is described in terms of a continuous spatial coordinate,  $z$ , which replaces the branching levels of the fractal tree from the aorta to the capillaries. As suggested by West [353], both the radii and the vessel lengths scale according to “cubic law” branching, i.e.,  $\rho_{k+1}/\rho_k = \mu_{k+1}/\mu_k = m^{-1/3}$ . These assumptions allow us to obtain the expression for the area  $\mathcal{A}(z)$  of the noncylindrical tube (Figure 8.5C) as a function of the coordinate  $z$ :

$$\mathcal{A}(z) = \frac{\pi \rho_0^2 \mu_0 \tilde{m}}{z(1 - \tilde{m}) + \mu_0 \tilde{m}}, \tag{8.9}$$

where  $\rho_0$  and  $\mu_0$  are the radius and the length of aorta, respectively, and  $\tilde{m} = m^{1/3}$ .

Further, a volume-preserving transformation allows the replacement of the varying radius tube with a tube of fixed radius  $\rho_0$  and fixed area  $\mathcal{A}_0 = \pi \rho_0^2$  (Figure 8.5D). This is accomplished by replacing  $z$  with a new coordinate  $z^*$  with the condition that the constant total flow of the fluid across a section is kept invariant under the transformation:

$$z = \frac{\mu_0 \tilde{m}}{\tilde{m} - 1} \left\{ 1 - \exp \left[ \frac{z^* (1 - \tilde{m})}{\mu_0 \tilde{m}} \right] \right\}. \tag{8.10}$$

### 8.6.2 Tracer Washout Curve

The disposition of a solute in the fluid as it flows through the system is governed by convection and dispersion. The convection takes place with velocity

$$v(z) = \frac{\mathcal{A}_0}{\mathcal{A}(z)} v_0, \tag{8.11}$$

where  $v_0$  is the velocity in the aorta and  $\mathcal{A}(z)$  is given by (8.9). If molecular diffusion is considered negligible, dispersion is exclusively geometric and consists of two components originating from the variance of the path lengths and of the vessel radii. Because the components are independent of each other, the global form of the dispersion coefficient is

$$D(z) = \left[ k_1 \sigma_{10}^2 + 2k_2 \sigma_{20}^2 \frac{\mu_0}{\rho_0} \right] \left[ \frac{\mathcal{A}_0}{\mathcal{A}(z)} \right]^2 v_0, \quad (8.12)$$

where  $k_1$  and  $k_2$  are proportionality constants, and  $\sigma_{10}^2$  and  $\sigma_{20}^2$  are the variances of the radius and the length of aorta, respectively [357, 360, 361]. The equation that describes the concentration  $c(z, t)$  of solute inside the tube is a convection–dispersion partial differential equation:

$$\frac{\partial c(z, t)}{\partial t} = \frac{\partial}{\partial z} \left[ D(z) \frac{\partial c(z, t)}{\partial z} \right] - v(z) \frac{\partial c(z, t)}{\partial z}$$

with  $D(z)$  and  $v(z)$  given by (8.12) and (8.11), respectively. Applying the transformation (8.10), the previous equation becomes a simple convection–dispersion equation with constant coefficients:

$$\frac{\partial c(z^*, t)}{\partial t} = D_0^* \frac{\partial^2 c(z^*, t)}{\partial z^{*2}} - v_0^* \frac{\partial c(z^*, t)}{\partial z^*}, \quad (8.13)$$

where

$$D_0^* = k_0 v_0, \quad v_0^* = \left( \tilde{m} \frac{k_0}{\mu_0} + 1 \right) v_0, \quad k_0 = k_1 \sigma_{10}^2 + 2k_2 \sigma_{20}^2 \frac{\mu_0}{\rho_0}.$$

These forms relate the dependence on the system characteristics. Equation (8.13) describes the concentration  $c(z^*, t)$  of a solute in a tree-like structure that corresponds to the arterial tree of a mammal. Considering also the corresponding venular tree situated next to the arterial tree and appropriate inflow and outflow boundary conditions, we are able to derive an expression for the spatiotemporal distribution of a tracer inside a tree-like transport network. We also make the assumption that the arterial and venular trees are symmetric, that is, have the same volume  $V$ ; then, the total length is  $L = V/\mathcal{A}_0$ . The initial condition is  $c(z^*, 0) = 0$  and the boundary conditions are:

- Inflow at  $z^* = 0$ :

$$\left[ -D_0^* \frac{\partial c(z^*, t)}{\partial z^*} + v_0^* c(z^*, t) \right] \Big|_{z^*=0} = \frac{q_0}{a_0} \delta(t)$$

where  $q_0$  is the dose, and  $\delta(t)$  is the Dirac delta function.

- Outflow at  $z^* = L$ :

$$\left. \frac{\partial c(z^*, t)}{\partial z^*} \right|_{z^*=L} = 0.$$

The outflow concentration  $c(L, t)$  of the above model describes tracer washout curves from organs that have a tree-like network structure, and it is given by an analytic form reported in [359].

### 8.6.3 Model for the Circulatory System

Based on the above, an elementary pharmacokinetic model considering the entire circulatory system was constructed. Thus, apart from the arterial and venular trees, a second set of arterial and venular trees, corresponding to the pulmonary vasculature, must be considered as well. These trees follow the same principles of (8.10) and (8.13), i.e., tubes of radius  $\rho_0$  are considered with appropriate length to accommodate the correct blood volume in each tree.

#### 8.6.3.1 Structure

An overall tube of appropriate length  $L$  is considered and is divided into four sequential parts, characterized as arterial, venular, pulmonary arterial, and pulmonary venular, Figure 8.6.

We assign the first portion of the tube length from  $z^* = 0$  to  $z^* = z_c^*$  to the arterial tree, the next portion from  $z^* = z_c^*$  to  $z^* = z_p^*$  to the venular, and the rest from  $z^* = z_p^*$  to  $z^* = L$  to the two symmetrical trees of the lungs. We consider that the venular tree is a structure similar to the arterial tree, only of greater, but fixed, capacity. Also, the two ends of the tube are connected, to allow recirculation of the fluid. This is implemented by introducing a boundary condition, namely  $c(0, t) = c(L, t)$ , which makes the tube ring-shaped. The “heart” is located at two separate points. The left ventricle-left atrium is situated at  $z^* = 0$ , and the right ventricle-right atrium is situated at  $z^* = z_p^*$ , Figure 8.6.

#### 8.6.3.2 Dispersion

Two separate values were used for the dispersion coefficient  $D_a$  for the arterial segment and  $D_p$  for the pulmonary segment. For the venular segment we consider that the dispersion coefficient has the value  $D_a(z_p^* - z_c^*)/z_c^*$ , meaning that it is proportional to the length of the segment. The flux preservation boundary condition,

$$D_p \left. \frac{\partial c(z^*, t)}{\partial z^*} \right|_{z^*=L} = D_a \left. \frac{\partial c(z^*, t)}{\partial z^*} \right|_{z^*=0},$$

must also be satisfied.

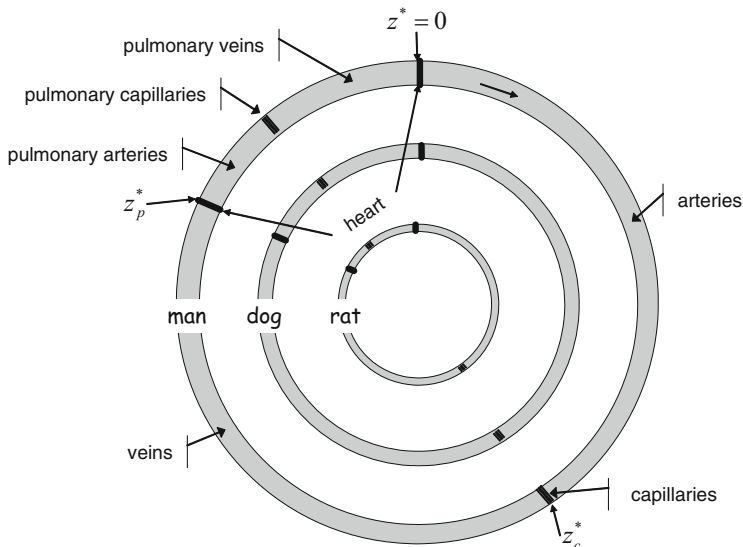


**Fig. 8.6** Schematic representation of the ring-shaped tube that models the circulatory system of a mammal. Blood flows clockwise. The tube is divided into segments corresponding to the arterial, venular, pulmonary arterial, and pulmonary venular trees

### 8.6.3.3 Elimination

The contribution of elimination of drugs is appreciable and is integrated into the model. A segment in the capillary region of the tube ( $z^* \approx z_c^*$ ) is assigned as the elimination site and a first-order elimination term  $kc(z^*, t)$  is now introduced in (8.13). The length of the elimination segment is arbitrarily set to  $0.02L$ , which is in the order of magnitude of the capillary length. The position of the elimination site is imprecise in physiological terms, but it is the most reasonable choice in order to avoid further model complexity.

### 8.6.3.4 Drug Administration and Sampling

The necessary initial condition for the intravenous administration of an exogenous substance,  $c(z^*, 0)$ , which is the spatial profile of  $c$  at the time of administration, is determined by the initial dose and the type of administration. This profile may have the shape of a “thin” Gaussian function if an intravenous bolus administration is considered, or the shape of a “rectangular” gate for constant infusion. The reference location  $z_0^*$  of this profile for an intravenous administration must be set close to the heart. Similarly, when lung administration is considered,  $z_0^*$  should be set in the capillary area of the lungs. Due to the geometric character of the model, a sampling site  $z_s^*$  should be either specified, in simulation studies, or calculated when fitting is performed.

The final model can be summarized as follows:

$$\frac{\partial c(z^*, t)}{\partial t} = \frac{\partial}{\partial z^*} \left[ D^*(z^*) \frac{\partial c(z^*, t)}{\partial z^*} \right] - v_0^* \frac{\partial c(z^*, t)}{\partial z^*} - W(z^*) k_c(z^*, t),$$

where  $W(z^*)$  is a combination of delayed in space Heaviside functions, i.e.,  $W(z^*) = H(z^* - z_c^* + 0.01L) - H(z^* - z_c^* - 0.01L)$ , and

$$D^*(z^*) = \begin{cases} D_a & \text{for } 0 < z^* \leq z_c^*, \\ D_a(z_p^* - z_c^*)/z_c^* & \text{for } z_c^* < z^* \leq z_p^*, \\ D_p & \text{for } z_p^* < z^* \leq L. \end{cases}$$

Boundary and initial conditions are considered as discussed above.

*Example 5. Indocyanine Green Injection*

The model was used to identify indocyanine green profile in man after a  $q_0 = 10$  mg intravenous bolus injection. Both injection and sampling sites ( $z_0^*$  and  $z_s^*$ , respectively) were closely located on the ring-shaped tube. The model of drug administration was a “thin” Gaussian function:

$$c(z^*, 0) = \frac{q_0}{V} \sqrt{\frac{b}{\pi}} \exp \left[ -b \left( \frac{z^*}{L} - \frac{z_0^*}{L} \right)^2 \right].$$

This administration corresponds to a bolus injection at the cephalic vein. The parameters set in the model were  $m = 3$ ,  $\mu_0 = 50$  cm,  $\mathcal{A}_0 = 3$  cm<sup>2</sup>, and  $b = 10^5$ . The estimated model parameters were:

- Structure:  $z_c^*/L = 0.28$ ,  $z_0^*/L = 0.83$ ,  $z_p^*/L = 0.85$ , and  $V = 4.41$ . These values result in  $L = 1470$  cm.
- Dispersion and elimination:  $D_a = 1826$  cm<sup>2</sup> s<sup>-1</sup>,  $D_p = 1015$  cm<sup>2</sup> s<sup>-1</sup>,  $v_0 = 44.98$  cm s<sup>-1</sup>, and  $k = 1.13$  s<sup>-1</sup>.

Figure 8.7 depicts the fitted concentration profile of indocyanine green at the sampling site along with the experimental data. ■

A one-dimensional linear convection–dispersion equation was developed with constant coefficients that describes the disposition of a substance inside a tree-like fractal network of tubes that emulates the vascular tree. Based on that result, a simple model for the mammalian circulatory system is built in entirely physiological terms consisting of a ring-shaped, one-dimensional tube. The model takes into account dispersion, convection, and uptake, describing the initial mixing of intravascular tracers. This model opens new perspectives for studies dealing with the disposition of intravascular tracers used for various hemodynamic purposes, e.g., cardiac output measurements [362, 363], volume of circulating blood determination [362], and liver function quantification [364]. Most importantly, the model can be expanded and used for the study of xenobiotics that distribute beyond the intravascular space.

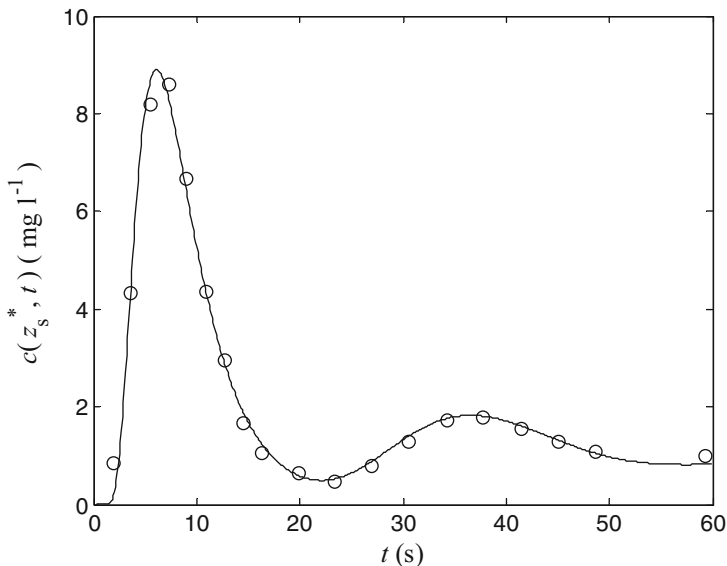


**Fig. 8.7** Indocyanine profile at the sampling location  $z_s^* = 1220$  cm after intravenous bolus administration of 10 mg. The peaks correspond to successive passes of the drug bolus from the sampling site as a result of recirculation. The dots indicate the experimental data

In future developments of the model, the positioning of organs that play an important role in the disposition of substances can be implemented by adding parallel tubes at physiologically based sites to the present simple ring-shaped model. Consequently, applications can be envisaged in interspecies pharmacokinetic scaling and physiologically based pharmacokinetic-toxicokinetic modeling, since both fields require a realistic geometric substrate for hydrodynamic considerations.

## 8.7 Compartmental Models and Heterogeneity

Initially, the deterministic theory was applied to describe the movement of a population of tracer molecules. Briefly, a drug administered as a bolus input into an organ modeled by homogeneous compartments results in a time–concentration curve describing the amount of the drug remaining in the organ as a function of the elapsed time of the form of a sum of exponential terms. Possibly because the individual molecules are infinitesimal in size, in most of the literature the implicit assumption is made of deterministic flow patterns. So, compartmental analysis, grounded on deterministic theory, has provided a rich framework for quantitative modeling in the biomedical sciences with many applications to tracer kinetics in general [365, 366] and also to pharmacokinetics [341]. The linear combinations of exponential function forms have provided a very rich class of curves to fit to time–concentration data, and compartmental models turn out to be good approximations for many processes.

Thus, compartmental models have been used extensively in the pharmacokinetic literature for some time, but not without criticism. These criticisms were directed:

- First, at the compartmental approach per se grounded on the assumption of homogeneous compartments. Compartmental models are in fact appropriate when there is an obvious partitioning of the material in the process into discrete portions, the compartments that exchange amounts of materials. From a theoretical standpoint, there has always been a consensus that the notion of a homogeneous compartment is merely a simplified representation for different tissues that are pooled together [367, 368].
- Second, at the fact that the models obtained are not necessarily exact because mixing in a compartment is not instantaneous. How good a compartment model is depends on the relative rates of mixing within a compartment as compared to the transfer rates between the compartments. Mixing may occur by diffusion, various types of convection, and combinations of them, so it is difficult to come up with a uniform theory of mixing. Ideally, we should measure the concentration of material throughout the process and define mixing in terms of the time course of a ratio such as the standard deviation divided by the mean concentration.
- Third, at the ill-conditioning of numerical problems for parameter estimation with models involving a large number of exponential terms. Wise [324] has developed a class of powers of time models as alternatives to the sums of exponentials models and has validated these alternative models on many sets of experimental data. From an empirical standpoint, Wise [269] reported “1000 or more” published time–concentration curves where alternative models fit the data as well or better than the sums-of-exponentials models.

Moreover, it is clear that even the continuous models are often unreliable models. Matter is atomic, and at a fine enough partition, continuity is no longer an acceptable solution. Furthermore, living tissues are made up of cells, units of appreciable size that are the basic structural and functional units of living things. And cells are not uniform in their interiors; they contain smaller units, the cellular organelles. There is inhomogeneity at a level considerably above the molecular. All these facts enhanced the criticism against determinism and the use of homogeneous compartments. More realistic alternatives have aimed at removing the limiting assumption of homogeneity:

- The process was considered as continuous and compartmental models were used to approximate the continuous systems [366]. For such applications, there is no specific compartmental model that is the best; approximation improves as the number of compartments is increased. In order to put compartmental models of continuous processes in perspective it may help to recall that the first step in obtaining the partial differential equation, descriptive of a process continuous in the space variables, is to discretize the space variables so as to give many *microcompartments*, each uniform in properties internally. The differential equation is then obtained as the limit of the equation for a microcompartment as its spatial dimensions go to zero. It is better to approximate the continuous processes with a finite-compartment system rather than go to the limit. In that

case, the partial differential equation is approximated by a set of simultaneous ordinary differential equations. In philosophy, compartmental modeling shares basic ideas with the finite element method, where the structure of the system is also used to define the elements of a partition of the system. But even if a finite-compartment approximation is used, how can we define the approximation error and its dependence on the size of the compartmental model? In addition, many compartmental models approximating continuous processes are so large that it may be difficult to deal with them and it may be useful or necessary to lump some of the compartments into one compartment. This raises a set of questions about the errors incurred in aggregation and about the optimal way of aggregating compartments.

- Noncompartmental models were introduced as models that allow for transport of material through regions of the body that are not necessarily well mixed or of uniform concentration [273]. For substances that are transported relatively slowly to their site of degradation, transformation, or excretion, so that the rate of diffusion limits their rate of removal from the system, the noncompartmental model may involve diffusion or other random-walk processes, leading to the solution in terms of the partial differential equation of diffusion or in terms of probability distributions. A number of noncompartmental models deal with plasma time–concentration curves that are best described by power functions of time.
- Physiological and circulatory models have been developed, and they have provided information of physiological interest that was not available from compartmental analysis. Rapidly, physiological models turned to the modeling of complex compartmental structures. In contrast, circulatory models associated with a statistical framework have proved powerful in describing heterogeneity in the process [271, 369]. Recently, the above presented complex model for the entire circulatory system was built, describing initial mixing following an intravascular administration in a tree-like network by a relatively simple convection–dispersion equation [359, 370].
- Stochastic compartmental analysis assumes probabilistic behavior of the molecules in order to describe the heterogeneous character of the processes. This approach is against the unrealistic notion of the “well-stirred” system, and it is relatively simpler mathematically than homogeneous multicompartment models. At first glance, this seems to be a paradox since the conventional approaches rely on the simpler hypothesis of homogeneity. Plausibly, this paradox arises from the analytical power of stochastic approaches and the unrealistic hypothesis of homogeneity made by compartmental analysis. Nevertheless with only a few exceptions, stochastic modeling has been slow to develop in pharmacokinetics and only recently have some applications also included stochastic behavior in the models.

In conclusion, compartmental models are generally well determined if there is an obvious partitioning of the material into compartments, and if the mixing processes within these compartments are considerably faster than the exchanges between the compartments.